Simultaneous 3D Imaging of Bone and Vessel Microstructure in a Rat Model: Measurement of Vascular-Trabecular Interdistance

Max Langer, Rhonda Prisby, Zsolt Peter, Alain Guignandon, Marie-Helene Lafage-Proust, Francoise Peyrin

Simultaneous 3D Imaging of Bone and Vessel Microstructure in a Rat Model: Measurement of Vascular-Trabecular Interdistance

Max Langer, Member, Rhonda Prisby, Zsolt Peter, Alain Guignandon,
Marie-Hélène Lafage-Proust, Françoise Peyrin, Fellow

***Abstract*—A method for simultaneous 3D imaging and analysis of microvascularization and bone microstructure in rat bone is presented. The method is based on the use of quantitative synchrotron micro-computed tomography (SR-μCT) coupled to an automatic image analysis procedure. Previously, analysis of bone microvascularization has generally been performed from 2D histology. The proposed method enables for the first time to simultaneously analyze in 3D the microvascularization and bone microstructure in a rat model. We also propose a new parameter, utilizing the availablilty of both microstructures to relate the two, which we dub the vascular-trabecular interdistance (VTI). The proposed method was applied to investigate the effect of intermittent parathyroid hormone (PTH) administration on angiogenesis and osteogenesis in rats. It was possible to extract 3D quantitative parameters both on bone microstructure and micro-vascularization. Due to the short acquisition times of SR-μCT and the efficiency of the image analysis algorithm, a large data set was analyzed, which permitted statistical analysis of the measured parameters. Statistical analysis showed that treatment with PTH significantly modulated several bone and vessel parameters, including the VTI.**

I. Introduction

Bone vascularization plays a major role in many physiological events such as fracture healing and bone growth, and pathological processes such as metastasis, Paget's disease and hematopoïetic disorders [1]. Moreover, bone blood supply has been recently shown to be involved in osteoporosis, the most frequent metabolic bone disease [2]. Further, the effects of anti-osteoporotic treatment on bone vascularization have yet to be investigated. The anatomical characterization of the bone vascular network was performed many years ago using 2D X-Ray imaging after intravascular opacification with contrast products in animal models [3].

M. Langer and F. Peyrin are with CREATIS-LRMN, CNRS UMR 5220; INSERM U630; Université de Lyon; INSA Lyon, F69621 Villeurbanne Cedex, France, and the European Synchrotron Radiation Facility, 6 rue Jules Horowitz, F38043 Grenoble, France (phone: +33-438-881977, e-mail: max.langer@esrf.fr).

Z. Peter was with CREATIS-LRMN and is now with University of Paris 10, PST/IUT of Ville d'Avray, GTE Department, 50 Rue de Sèvres, F-92410 Ville d'Avray, France.

R. Boistel is with the ESRF and Museum National d'Histoire Naturelle, Départ. EGB, CNRS UMR 7179, 57 rue Cuvier, F-75231 Paris, France

R Prisby and MH Lafage Proust are with Université de Lyon, St-Etienne, F-42023 France ; Inserm, U890, F-42023 France.

R. Prisby is also with the Dept. of Kinesiology, University of Texas as Arlington, TX 76019, USA

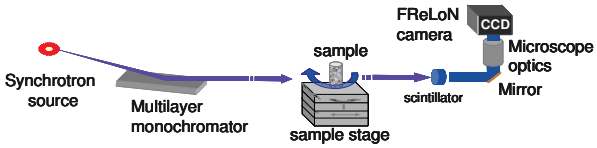

Fig. 1. Schematic of the imaging setup [6]. Monochromatic X-rays at 25 keV were selected from undulator radiation with a single reflection multilayer monochromator. Samples were mounted on a sample stage (3D translations and rotation) for tomographic imaging. A FreLoN [8] camera was used for detection.

Other data were provided by histological analyses of vessels in bone [4]. Bone microstructure has been extensively investigated using micro-computed tomography (μCT) [5]. However, these methods have not permitted precise quantification and imaging of the vascular network in three dimensions (3D), nor did they permit a full analysis of the spatial relationships between bone and vascular system. These studies focused on analyzing either bone micro-structure or microvascularization separately.

The purpose of this work was to develop a new method in order to quantify simultaneously the 3D organization of bone microstructure and microvascularization in a rat model. To this end, we used synchrotron radiation 3D micro-computed tomography (SR-μCT) at the European Synchrotron Radiation Facility (ESRF), Grenoble, France [6]. Due to the high flux of third generation synchrotron sources, SR-μCT is a quantitative CT technique allowing to reach micrometric spatial resolution [7]. Imaging was performed on rat samples posthumously injected with a contrast agent at a high spatial resolution (voxel size 2.8μm) to correctly resolve the microvasculature. An automatic image analysis method was then developed to identify cortical and trabecular bone envelopes, and bone and vascular structure within each envelope, Characteristic 3D quantitative parameters were then extracted from both microstructures.

Since we now have access to both bone and vascular microstructures simultaneously, it is interesting to quantify their spatial relationship. We do this by introducing a new parameter, which we dub the vascular-trabecular interdistance (VTI), which we define as the average local distance between vessels lying in the trabecular bone region to the trabeculae.

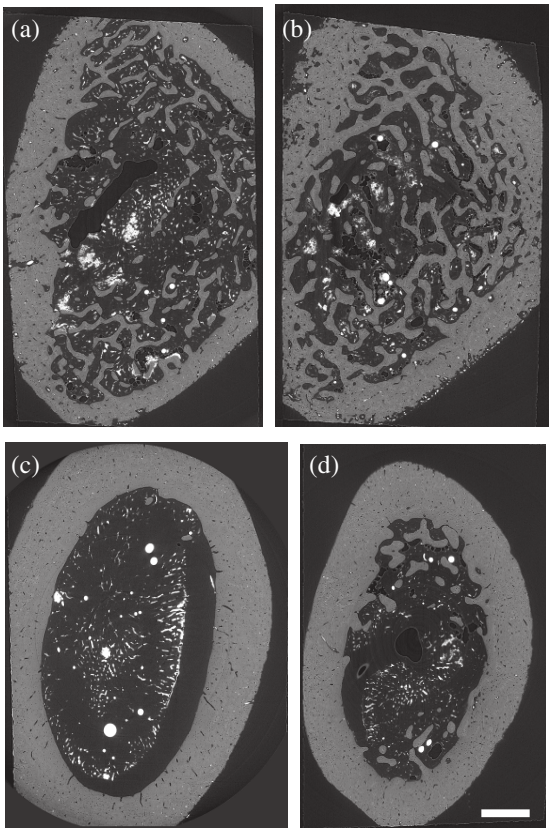

Fig. 2. Tomographic slice through a femur of a rat injected with contrast agent and embedded in methylmethacrylate (MMA): (a) control sample, ROI1, (b) PTH sample, ROI2, (c) control sample, ROI2, (d) PTH sample, ROI2 All phases are visible on the slice: vessels brightest (due to the contrast agent), bone as light grey, acetate as dark gray and air as black. The scale bar corresponds to 1 mm.

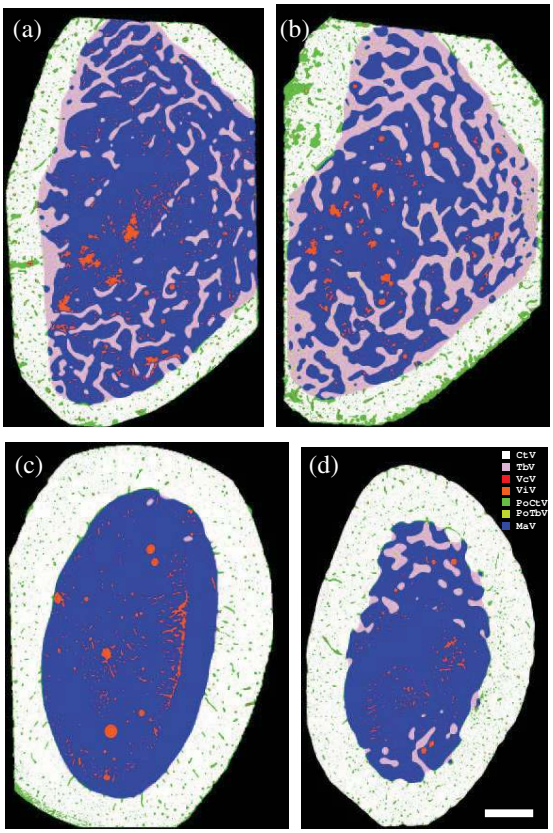

Fig. 3. Labelled volume consisting of the different segmented volumes: (a) control sample, ROI1, (b) PTH sample, ROI2, (c) control sample, ROI2, (d) PTH sample, ROI2. All desired bone parameters can be calculated based on this volume.

The method was applied to investigate the effect of the potentially anti-osteoporotic agent parathyroid hormone (PTH) on the bone and vascular networks in rats. Quantitative parameters were computed from 28 3D images corresponding to 14 rat femur samples Statistical analysis revealed that treatment with PTH significantly increased bone volume and thickness, decreased bone mineralization and increased average vessel thickness. Treatment with PTH also significantly decreased the VTI, which implies a spatial reorganization of the vessels to grow closer to the trabeculae. The method allowed for the first time to analyze quantitatively both microvasculature and bone tissue.

II. Materials and Methods

A. Sample preparation

Rats were given either PTH (sc, 100 µg/kg/day) for 5 days per week for 4 weeks or placebo (0.9 % saline). Following euthanization, the rats were subsequently infused with a barium sulfate solution (contrast agent). The femora were dissected, fixed in 10 % paraformaldehyde for 3 days, then transfered to and stored in 100 % acetone, and subsequently embedded in methylmethacrylate (MMA). Of these embedded femora small sub-samples (parallelepiped side ~4mm) were cut for imaging.

B. Image acquisition

3D SR-µCT imaging was performed on beamline ID19 at the ESRF, where a parallel beam 3D µCT setup has been developed [6] (Fig. 1). It consisted in recording 2000 radiographs of the sample under different angles of view over 360° using a FreLoN camera: a 2048x2048 pixel CCD-based detector [8]. The imaging system was set up to give a pixel size of 2.8 µm.on the detector, yielding a cylindrical field of view (FOV) of diameter 5.6 mm. The energy was set to 25 keV, selected from undulator radiation using a single reflection multilayer monochromator, giving a beam height of approximately 2 mm. Exposure time was set to 0.25 s per image to ensure a large dynamic range (the detector provides 14 bits). The acquisition time for one scan was about 18 minutes.

For each sample, two images corresponding respectively to a region of interest in the metaphysis (ROI1) and diaphysis (ROI2) were acquired. The ROI1 was scanned in the IISP. Since at this level the sample did not fit the FOV, we used a non-conventional acquisition procedure, recording

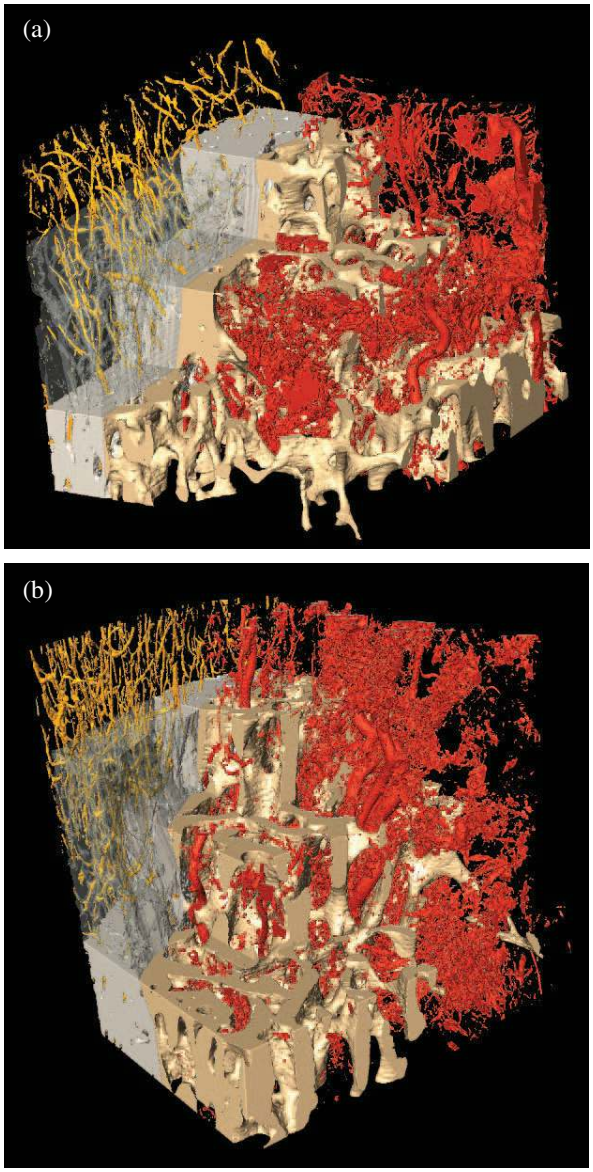

Fig. 4. Volume rendering showing bone and vessel compartments in ROI1. (a) control sample, (b) PTH sample. Note the apparent increase of vessel and trabecular thickness in the PTH sample. This is supported by the quantitative findings (Fig. 4, Tab. I).

images over 360° with the axis of rotation displaced to the edge of the FOV, thus enabling the reconstruction of a larger FOV which encompasses the sample. This procedure yielded reconstructed 3D images of 2500x2500x700 voxels.

C. Image segmentation

The segmentation step requires identifying vessels, bone and back-ground. In addition, since it was desired to separately analyze trabecular and cortical bone, trabecular and cortical bone envelopes had to be labeled.

Segmentation of bone and vessels was performed using 3D region growing based on a gray level criterion. Separating the trabecular and cortical bone compartments

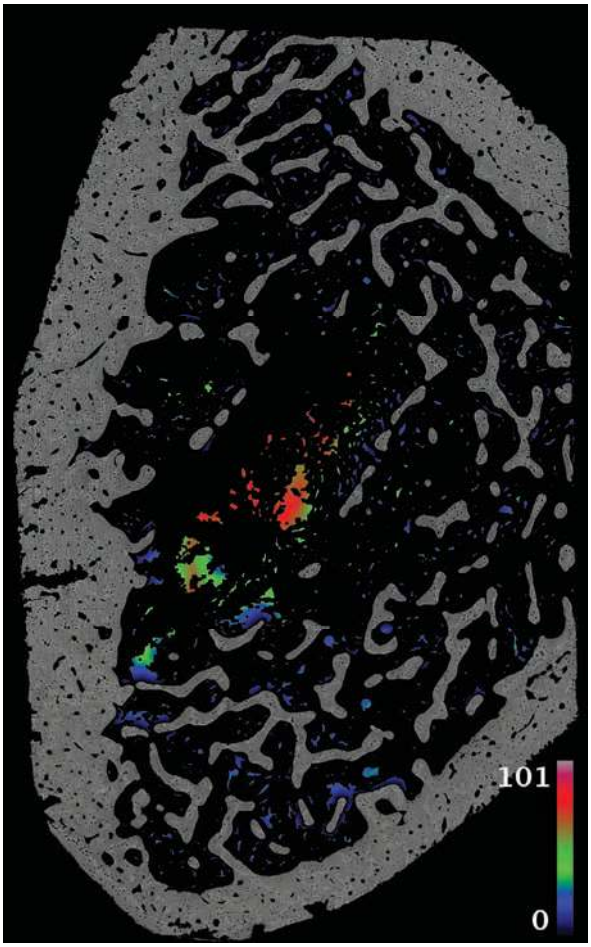

Fig. 5. Measurement of the vascular-trabecular interdistance (VTI). The 3D distance map from background to Tb is multiplied with Vi to yield the distance to Tb in each point in Vi. The figure shows a 2D slice of this distance map, color corresponding to distance in µm, superimposed over the bone volume, shown in in grayscale.

automatically was not straightforward, since there was no measurable difference in grayscale between the two types of bone. In ROI2, it was observed that the cortical bone generally has a thicker cross-section. Segmentation of cortical bone could therefore be performed by first filling pores in the bone volume with a median filter, then calculating and thresholding the 3D local thickness map [9,10]. This yields the envelope of the cortical bone. This volume can then be used to separate bone into trabecular and cortical bone, and vessels into cortical and internal vessels by arithmetical operations. The total volume is calculated by filling in pores in the bone volume with a median filter, then filling in the empty space spanned by the bone.

There are specific problems in this study that needed to be addressed. The high resolution enables imaging of the vascularization, but also allows to resolve pores (lacunae) in both cortical and trabecular bone. The recorded volumes to be treated are very large due to the large detector size. This

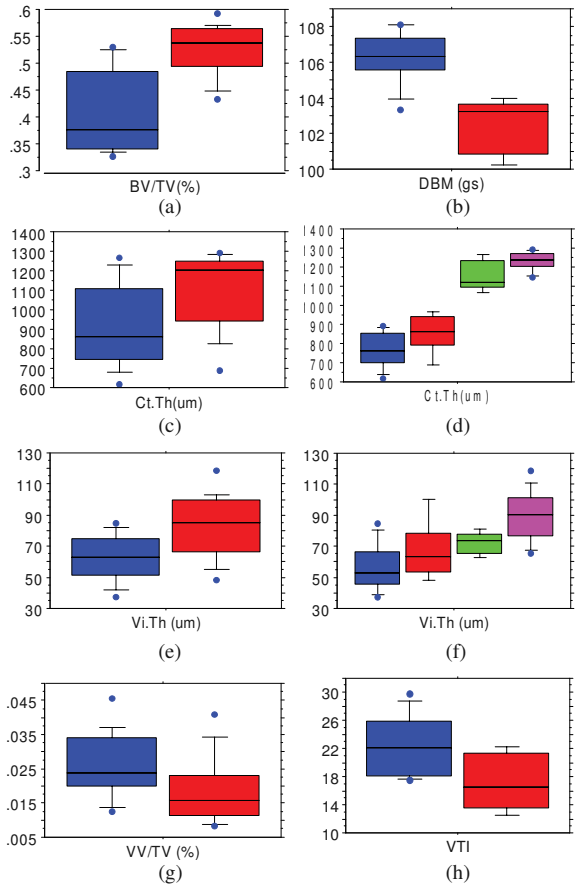

Fig. 6. Box plots of selected bone parameters (control in blue, PTH in red). Several observations can be made, which are shown to be significant with a non-paired t-test. (a) PTH increases BV/TV (b) PTH reduces DBM in ROI1 (c) PTH increases Ct.Th (d) PTH decreases VV/TV (e) PTH increases ViV.Th and (f) PTH increases Vi.Th in ROI2 but not significantly in ROI1 (ROI1 in blue/red, ROI2 in green/magenta).

puts stringent requirements on time and memory complexity of the image processing algorithm.

After segmentation, each volume was partitioned into seven sub-volumes (Fig. 3): Cortical volume, Trabecular volume, Pore volume in cortical bone, Pore volume in trabecular bone, Vessel volume in cortical volume, Vessel volume in Inner volume, Marrow Volume. 3D renderings of bone and vessel volumes are shown in Fig. 4.

D. Extraction of quantitative parameters

From this splitting, it was possible to recover all other desired subvolumes. For instance the cortical bone envelope is the union of the cortical volume, pore volume in cortical bone and vessel volume in cortical volume.

Several parameters were extracted from the segmented volumes. The volume of each compartment was directly measured by counting voxels. The measured volumes are

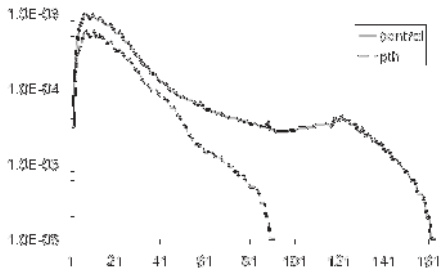

Fig. 7. Histograms of $d(x \in \mathrm{Vi}, \mathrm{Tb})$ for a sample treated with PTH and a control sample.

- Total volume (TV): volume spanned by the outer contour of the cortical bone
- Inner volume (IV): volume spanned by the inner contour of the cortical bone
- Bone volume (BV)
- Cortical volume (CtV)
- Cortical envelope volume (CtMV): volume of cortical bone with porosity filled in
- Trabecular volume (TbV)
- Trabecular envelope volume (TbMV): volume of trabecular bone with porosity filled in
- Total vessel volume (VV)
- Vessel volume inside cortical envelope (VcV)
- Vessel volume inside inner volume (ViV)
- Marrow volume (MaV)
- Pores in cortical bone (PoCtV)
- Pores in trabecular bone (PoTbV)

To allow for comparison between samples, normalized ratios are calculated:

- Bone ratios: BV/TV, CtV/TV, CtMV/TV, TbV/IV, TbMV/IV
- Vessel ratios: VV/TV, VcV/CtV, ViV/IV, ViV/MaV
- Lacunar ratios: PoCtV/CtMV, PoTbV/TbMV
- Marrow ratio: MaV/TV

Based on the segmented volumes, more complex parameters have also been extracted. Local thickness of bone and vessel compartments are calculated, yielding

- Mean cortical thickness (Ct.Th)
- Mean trabecular thickness (Tb.Th)
- Mean vessel thickness (V.Th)
- Mean thickness of internal vessels (Vi.Th)
- Mean thickness of cortical vessels (Vc.Th)

By multiplying the segmented bone compartment with the grayscale volumes, only the bone part of the grayscale images is extracted. This gives access to the bone mineralization levels, which yields the mean degree of mineralization of bone (DMB).

TABLE I
HYPOTHESES SIGNIFICANT AT 5% LEVEL

Hypothesis	p-number
PTH increases BV/TV	0.0001
PTH increases CtMV/TV in ROI2	0.0455
PTH increases TbMV/IV in ROI1	<0.0001
PTH increases TbV/IV in ROI1	<0.0001
PTH increases Ct.Th	<0.0001
PTH increases Tb.Th in ROI1	<0.0001
PTH decreases MaV/TV	<0.0001
PTH decreases DMB in ROI1	0.0003
PTH decreases VV/TV	0.0451
PTH increases Vi.Th	0.0040
PTH decreases VTI	<0.0001

E. Vascular-Trabecular Interdistance (VTI)

Since we now have access to both bone and vessel microstructures simultaneously, it seems reasonable to define a measure that relates the two quantitatively. Therefore, we propose a new parameter relating to both bone and vessels. It is defined as the average of the local distance from each point in the Vi compartment to the Tb compartment, and we designate it the vascular-trabecular interdistance (VTI).

Let $\mathbf{Z}^3$ be a three-dimensional discrete space, and X an object in $\mathbf{Z}^3$. Let $d(x,x')$ be a discrete distance between two points in $\mathbf{Z}^3$. We use here the (3,4,5) Chamfer distance [11] which has been shown to be a good approximation of the Euclidean distance [12]. The distance transform DT, defined from $\mathbf{Z}^3$ to $\Re^+$, associates to each voxel its distance to the complement of X (denoted $\neg X$):

$$\mathrm{DT}(x) = d(x, \neg X) = \inf\{ d(x,y) / y \in \neg X \} \quad (1)$$

Assuming that the relevant compartments, trabecular bone (Tb) and internal vessels (Vi) have been segmented from the data, so that Tb and Vi are binary volumes, the first step in calculating VTI is to calculate the distance transform from background to trabecular bone, DT(¬Tb). This is then multiplied pointwise with Vi to yield the distance map from each point in Vi to Tb, that is d(x). A 2D slice through this distance map is shown in Fig. 5. VTI can the be defined as the average distance from Vi to Tb as

$$\mathrm{VTI} = \sum_{x \in \mathrm{Vi}} d(\mathrm{x}, \mathrm{Tb}) / |\mathrm{Vi}|,$$

where $|\cdot|$ denotes cardinality.

F. Statistical analysis

Statistical testing was performed between the two groups on all measured parameter, both in each ROI separately and the two ROIs combined. The two-sample unpooled t-test was used in all cases. Differences between the two groups were considered statistically significant at the 5 % level ($p<0.05$).

III. RESULTS

In total, 28 samples were analyzed, 13 controls and 15 from the PTH group. Significant differences between the two are reported in Tab. I. Box plots of a selection of important parameters are shown in Fig. 6. The following significant differences could be observed between the two groups

Bone volume. PTH treated rats had 30 % higher bone ratio ($p<0.0001$), 40 % higher in ROI1 ($p<0.0001$) and 10 % higher in ROI2 ($p=0.0364$). PTH treated rats had 70 % greater trabecular volume ratio ($p<0.0001$) and trabecular envelope ratio ($p<0.0001$), both in ROI1. PTH treated rats also had a slightly higher cortical envelope ratio in ROI2 ($p=0.0455$).

Bone thickness: Rats treated with PTH showed a 50 % increase in cortical thickness ($p<0.0001$) and 30 % increase in trabecular thickness in ROI1 ($p<0.0001$).

Bone mineralization: the control group showed 10 % higher average mineralization in ROI1 ($p=0.0003$).

Marrow volume: PTH treated rats showed a 20 % decrease of marrow volume ratio ($p<0.0001$)

Total Vessel Volume: PTH treated rats showed a decrease in vessel volume by 27 % ($p=0.0451$).

Vessel thickness: PTH treated rats showed an increase in thickness of the internal vessels by 30 % ($p=0.0040$).

Vascular-trabecular interdistance: Rats treaded with PTH showed a 24 % decrease in VTI ($p<0.0001$).

IV. DISCUSSION AND CONCLUSION

SR-μCT allowed for the first time to study simultaneously bone microstructure and microvascularization at very high spatial resolution. Due to adapted image analysis, it was possible to extract from the data a large number of 3D quantitative parameters. A new parameter was also defined, the vascular-trabecular interdistance (VTI) which relates the bone and vascular microstructures. This parameters can be viewed as quantifying the spatial organization of the micro-vascularization relative to the trabecular structure.

The method was applied to study the effect of PTH treatment on bone microvascularization. The results demonstrated that PTH modulated both bone and vascular parameters (e.g. BV/TV, TbV, CtV, V.Th, etc.). The increases in bone volume and trabecular and cortical thicknesses are in agreement with previous studies. Further, the 3D vessel thicknesses were also significantly increased with PTH treatment. SR μCT also permitted the analysis of the degree of bone mineralization in 3D, which was diminished with intermittent PTH administration. The VTI was also strongly modulated due to PTH treatment. The decrease in VTI can be interpreted as vessels growing closer to the trabecular wall. This could imply an increased oxygen transport to the bone

We acknowledge that the number of samples analyzed is limited at present. Further data has been acquired and will be analyzed with the present methods to augment the number of samples and make the statistical analysis more robust. Further work also includes adaptation of the method to mouse bone, which sets different requirements on the whole chain, from contrast agent to imaging setup and data analysis.

REFERENCES

[1] B. Arora, R. Mesa, and A. Tefferi, "Angiogenesis and anti-angiogenic therapy in myelofibrosis with myeloid metaplasia," *Leuk. Lymphoma,* vol. 45, pp. 2373-2386, 2004.

[2] J. F. Griffith, D. K. Yeung, P. H. Tsang, K. C. Choi, T. C. Kwok A. T. Ahuja, K. S. Leung, and P. C. Leung, "Compromized bone marrow perfusion in osteoporosis," *J. Bone Miner. Res.,* vol. 23, pp. 1068-1075, 2008.

[3] F. H. Sim, and P. J. Kelly, "Relationship of bone remodeling, oxygen consumption, and blood flow in bone," *J. Bone Joint Surg. Am.,* vol. 52, pp.1377-1389, 1970.

[4] Z. Yao, M. H. Lafage-Proust, J. Plouët, S. Bloomfield, C. Alexandre, and L. Vico, "Increase of both angiogenesis and bone mass in response to exercise depends on VEGF," *J. Bone Miner. Res.,* vol. 19, pp. 1471-1480, 2004.

[5] R. Müller, "Hierarchical Microimaging of Bone Structure and Function," *Nat. Rev. Rheumatol.*, vol.. 5, pp. 375-381, 2009.

[6] M. Salomé, F. Peyrin, P. Cloetens, C. Odet, A.-M. Laval-Jeantet, J. Baruchel, and P. Spanne, "A Synchrotron Radiation Microtomography System for the Analysis of Trabecular Bone Samples," *Med. Phys*., vol. 26, pp. 2194-2204, 1999.

[7] S. Nuzzo, F. Peyrin, P. Cloetens, J. Baruchel and G. Boivin, "Quantification of the degree of mineralization of bone in three dimensions using synchrotron radiation microtomography," *Med Phys*, vol/ 29, pp. 2672-2681, 2002.

[8] J.-C Labiche, O. Maton, S. Pascarelli, M. A. Newton, G. C. Ferre, C. Curfs, G. Vaughan, A. Homs, and D. F. Carreiras, "The FReLoN Camera as a Versatile X-ray Detector for Time Resolved Dispersive EXAFS and Diffraction Studies of Dynamic Problems in Materials Science, Chemistry, and Catalysis," *Rev. Sci. Instrum*., vol. 78, pp. 091301, 2007.

[9] T. Hildebrand and P. Rüegsegger, "A New Method for the Model-independent Assessment of Thickness in Three-dimensional Images," *J. Microsc*., vol. 185, pp. 67-75, 1997.

[10] E. Martín-Badosa, A. Elmoutaouakkil., S. Nuzzo, D. Amblard, L. Vico, and F. Peyrin, "A method for the automatic characterization of bone architecture in 3D mice microtomographic images," Computerized Medical Imaging and Graphics, vol. 27, pp. 447-458, 2003.

[11] U. Montanari, "Continuous skeletons from digitized images", *JACM*, vol. 16, pp. 534-549, 1969

[12] G. Borgefors, "Distance transformations in Arbitrary dimensions", *Comput. Vis. Graph. Im. Proc*., vol. 27, pp. 321-345, 1984